Extracting the Density Profile of an Electronic Wave Function in a Quantum Dot

Extracting the density profile of an electronic wavefunction in a quantum dot

Erin E. Boyd[1] and Robert M. Westervelt[1,2]

[1]Department of Physics, Harvard University, Cambridge, MA 02138, USA

[2]School of Engineering and Applied Science, Harvard University, Cambridge, MA 02138, USA

PACS: 07.79.-v, 73.23.Hk, 73.63.Kv, 73.63.Nm

ABSTRACT

We use a model of a one-dimensional nanowire quantum dot to demonstrate the feasibility of a scanning probe microscope (SPM) imaging technique that can extract both the energy of an electron state and the amplitude of its wavefunction using a single instrument. This imaging technique can probe electrons that are buried beneath the surface of a low-dimensional semiconductor structure and provide valuable information for the design of quantum devices. A conducting SPM tip, acting as a movable gate, measures the energy of an electron state using Coulomb blockade spectroscopy. When the tip is close to the nanowire dot, it dents the wavefunction $\Psi(x)$ of the quantum state, changing the electron's energy by an amount proportional to $|\Psi(x)|^2$. By recording the change in energy as the SPM tip is moved along the length of the dot, the density profile of the electronic wavefunction can be found along the length of the quantum dot.

I. INTRODUCTION

As electronic devices become smaller, quantum mechanical effects become central to their operation. Knowledge of the energy levels and electronic wavefunctions will be crucial to design and understand quantum devices for applications ranging from beyond-CMOS electronics to quantum information processing. Scanning probe microscope (SPM) techniques provide valuable information about the spatial behavior of electrons in nanostructures. A scanning tunneling microscope (STM) images electrons on the surface of a structure at the atomic scale. Using a cooled STM, electron waves in an elliptical resonator on a copper surface were imaged,[1,2] the wavefunctions of electrons in a metallic single-walled carbon nanotube were measured,[3] and the phases of an electron eigenstate in an enclosed region on a copper surface were mapped.[4] The conducting tip of a cooled SPM has been used as a moveable gate to capacitively probe electrons inside nanostructures to image the flow of electron waves from a quantum point contact[5-9] and through a quantum ring[10-12] and to measure the energy of quantum states.[13-18]

Semiconductor nanostructures are attractive for quantum devices. Few electron quantum dots made from GaAs/AlGaAs heterostructures that contain only a few electrons have well-defined quantum states that can be measured with Coulomb blockade spectroscopy[19,20] and coupled quantum dots can be used for quantum information processing.[21] Semiconductor nanowires confine the electrons laterally, quantizing their motion into discrete subbands and providing close lateral access.[22] Quantum dots can be defined by grown-in barriers in a nanowire heterostructure.[23-26] A very narrow nanowire can line up electrons into a single row, to form a one-dimensional (1D) electron gas.[18]

A major challenge for developers of quantum devices is to obtain information about the electronic wavefunction of quantum states in the interior of devices. Suggested techniques include a grown-in potential perturbation,[27] changing the phase with the vector potential of an applied magnetic field,[28] and a potential perturbation from an external probe.[29]

In this paper, we propose an imaging technique to measure the energy levels of an electron inside a nanostructure and to extract the density profile of the electronic wavefunctions using a cooled SPM. The nanostructure chosen to illustrate the imaging techniques is a long InAs quantum dot formed by two tunnel barriers along an otherwise uniform nanowire.[18,24,25] With a suitably narrow nanowire, only the lowest subband is occupied and the electrons form a 1D system. Figure 1 shows a schematic diagram of the SPM setup, including the nanowire with source and drain contacts, a SiO_2 insulating layer, and a conducting backgate. Serving as a moveable gate, a conducting tip is scanned at a constant height along the nanowire, while the sample conductance G is mapped *vs*. SPM tip position x_{tip}. The weakly charged SPM tip locally dents the wavefunction $\Psi_N(x)$ of a state, causing a change $\Delta E_N(x_{tip})$ in energy E_N of the quantum state as the tip is moved along the sample. Using first-order perturbation theory, the density profile $|\Psi_N(x)|^2$ of the electronic wavefunction can be extracted from the energy map $\Delta E_N(x_{tip})$, which is measured using Coulomb blockade spectroscopy. This imaging technique could be used to study the transition between the Wigner Crystal and the Luttinger Liquid states predicted by Qian *et al.* (2010) in Ref. 30. The imaging technique we propose in this paper combines Coulomb blockade transport measurements with a weakly perturbing SPM tip to perform energy level spectroscopy and wavefunction diagnostics with the same system.

II. IMAGING TECHNIQUE

A. Model

Figure 1 is a schematic diagram that shows how a cooled SPM can image the density profile $|\Psi_N(x)|^2$ of an electron wavefunction inside a long, thin InAs quantum dot defined by two tunnel barriers in an otherwise uniform InAs nanowire. Nanowires are attractive candidates for imaging their density profile, because the tip can approach very close to the buried electrons. This wavefunction extraction technique is also valid for other electron gas systems. Figure 1 shows a conducting SPM tip, with radius of curvature R_{tip} = 20 nm, scanned along the length of the nanowire with the bottom of the tip at a height H_{tip} above the top of the nanowire. A constant voltage V_{tip} is applied between the SPM tip and the nanowire. With the source grounded, the backgate voltage V_{bg} applied to the conducting substrate tunes the average electron density. The conducting SPM tip acts as a moveable gate to capacitively probe the energy of electron states using Coulomb blockade spectroscopy by recording the conductance G as the tip is moved along the nanowire. [13-16,18]

The geometry of the SPM tip potential and electron states in the sample are important for the proposed wavefunction imaging technique. The spatial width of the tip potential perturbation $\Phi_{tip}(x-x_{tip})$ created inside the nanowire is determined by the height of the tip above the nanowire axis. This width must be comparable to the spatial separation of features in $|\Psi_N(x)|^2$ to image the wavefunction, [31] as discussed below. We simplify the analysis by assuming the nanowire quantum dot is effectively 1D, with only one radial state occupied, and that changes in the

wavefunction $\Psi_N(x)$ occur only along the length of the nanowire, labeled the x-axis. In this paper, we ignore electron-electron interactions and assume each electron level can only be occupied by one electron, ignoring spin degeneracy. These assumptions can be relaxed for the analysis of a real system, and this method can operate as an experimental diagnostic tool to supply information about the amplitude of an unknown arbitrary wavefunction. For the analysis presented below, we examine an ultra-thin InAs quantum dot with diameter d_{dot} = 30 nm and length L_{dot} = 300 to 500 nm defined by tunnel barriers in an otherwise uniform InAs nanowire. The large aspect ratio L_{dot}/d_{dot} > 10 allows access to the spatial features of the density profile $|\Psi_N(x)|^2$ as the first few electrons are loaded onto the dot.

B. Imaging mechanism

Figure 2 demonstrates how to extract the density profile $|\Psi_N(x)|^2$ of a wavefunction from the change in energy $\Delta E_N(x_{tip})$ of the corresponding state as the SPM tip is moved along the nanowire quantum dot. The shape of the tip potential $\Phi_{tip}(x\text{-}x_{tip})$ can be calculated from Maxwell's equations, and the energy change $\Delta E_N(x_{tip})$ along the dot can be provided by an experimental measurement. The first column in Fig. 2 shows the density profile $|\Psi_N(x)|^2$ for a rectangular quantum well along a 1D wire. The values of $|\Psi_N(x)|^2$ in Figs. 2(a) to 2(c) are the normalized wavefunctions for the ground state (N = 1) and first excited states (N = 2, 3) :

$$\Psi_N(x) = \sqrt{2 / L_{dot}} \sin\left(\frac{N\pi x}{L_{dot}}\right). \tag{1}$$

While square well wavefunctions are used to demonstrate the imaging technique, this method will supply information about the amplitude of an arbitrary wavefunction.

The tip potential Φ_{tip} used to probe the wavefunction is found by modeling the tip as a charged metal sphere above a dielectric plane and adding an appropriate scaling factor. From the method of image charges, the first order term of the electric potential $\Phi_{tip}(x)$ from a charged metal sphere that is held at a fixed position above a dielectric slab on a metal sheet is: [31]

$$\Phi_{tip}(x) = \frac{Q_{eff}}{\varepsilon_{eff}\sqrt{x^2 + (cd_{total})^2}}, \tag{2}$$

where Q_{eff} is the effective charge on the spherical tip, ε_{eff} is the effective relative permittivity of the region of the measurement, d_{total} is the total distance from the center of the spherical tip to the metal sheet, and c is a scaling factor for d_{total}. To find the tip potential $\Phi_{tip}(x)$ at the metal sheet with no nanowire present $c = 1$.

The tip potential $\Phi_{tip}(x)$ at the conducting backgate if a nanowire quantum dot is present is given by:

$$\Phi_{tip}(x) = \frac{Q_{eff}}{\varepsilon_{eff}\sqrt{x^2 + \left[c(d_{dot} + H_{tip} + R_{tip} + l_{ox})\right]^2}}, \tag{3}$$

where H_{tip} is the height from the bottom of the tip to the top of the nanowire (H_{tip} = 10 nm) and l_{ox} is the thickness of the dielectric oxide layer (l_{ox} = 10 nm). Since the quantum dot will only contain a few electrons when measuring the wavefunction, the presence of the dot will not noticeably effect the potential distribution from the tip. However, the electrons in the dot will experience a narrower tip potential than at the backgate, since the quantum dot is closer to the tip. This is accounted for by the scaling factor c. To find c, we modeled the electrostatic setup, including the backgate, dielectric layer, InAs quantum dot and leads, and metallic spherical tip, using finite-element modeling software. Fitting the software's result to Eq. 3, we find $c \approx 0.64$. The corresponding tip potential $\Phi_{tip}(x)$ used in this paper is plotted in Figs. 2(d) to 2(f).

From first-order perturbation theory, the change in energy $\Delta E_N(x_{tip})$ in the quantum dot of an electron wavefunction dented by the SPM tip is the expectation value of the perturbing tip potential $\Phi_{tip}(x - x_{tip})$ for the unperturbed wavefunction $\Psi_N(x)$:

$$\Delta E_N(x_{tip}) = \left\langle \Psi_N(x) \middle| e\Phi_{tip}(x - x_{tip}) \middle| \Psi_N(x) \right\rangle = e\int_{-\infty}^{\infty} |\Psi_N(x)|^2 \Phi_{tip}(x - x_{tip})dx. \quad (4)$$

This approximation is valid as long as the strength of the tip potential is small compared to the potential of the dot. [29] Therefore, the change in energy of the dot $\Delta E_N(x_{tip})$, plotted in Figs. 2(g) to 2(i), can be found by convolving the density profile $|\Psi_N(x)|^2$ with $e\Phi_{tip}(x)$:

$$\Delta E_N(x_{tip}) = e\int_{-\infty}^{\infty} |\Psi_N(x)|^2 \Phi_{tip}(x - x_{tip})dx = \left|\Psi_N(x)\right|^2 * (e\Phi_{tip}(x)), \quad (5)$$

where $*$ denotes the convolution function. From the convolution theorem, [32] the Fourier transforms of these quantities follow the following expression:

$$\Im[\Delta E_N(x_{tip})] = \Im[|\Psi_N(x)|^2] \; \Im[e\Phi_{tip}(x)]. \quad (6)$$

Therefore, the extracted density profile $|\Psi_N(x)|_{ext}^2$ can be obtained from a measurement of $\Delta E_N(x_{tip})$ by taking the following inverse Fourier transform:

$$|\Psi_N(x)|_{ext}^2 = \Im^{-1}\left(\Im[\Delta E_N(x_{tip})] / \Im[e\Phi_{tip}(x)]\right), \quad (7)$$

where the tip potential $\Phi_{tip}(x)$ is known from theory or an independent measurement. The extracted density profile $|\Psi_N(x)|_{ext}^2$, shown in Figs. 2(j) to 2(l), agrees with the original density profile $|\Psi_N(x)|^2$ shown in Figs. 2(a) to 2(c). Information extracted with this imaging technique will allow a fuller understanding of electrons in quantum devices.

C. Resolution

When performing the wavefunction extraction experiment on a device, the signal to noise ratio of $\Phi_{tip}(x - x_{tip})$ and $\Delta E_N(x_{tip})$, the width of $\Phi_{tip}(x - x_{tip})$ compared with the spatial features of the wavefunction $|\Psi(x)|^2$, and the temperature T all influence the resolution of the extracted wavefunction $|\Psi_N(x)|_{ext}^2$. The width of the Coulomb blockade conductance peaks increases with temperature,[33] and $\Delta E_N(x_{tip})$ can be measured more accurately at lower T.

The width of the tip potential $\Phi_{tip}(x - x_{tip})$ seen by the electrons is influenced by the separation between the electrons and the tip. Figure 3 shows the effect of different tip heights H_{tip} = 10 nm, 20 nm, and 40 nm on the shape of the $\Delta E_2(x_{tip})$ profile for a dot with N = 2 electrons and diameter d_{dot} = 30 nm. Figures 3(a) to 3(c) plot $\Delta E_2(x_{tip})$ *vs*. x_{tip} for a dot of length L_{dot} = 300 nm, while Figs. 3(d) to 3(f) plot $\Delta E_2(x_{tip})$ *vs*. x_{tip} for L_{dot} = 500 nm. As expected smaller tip heights H_{tip} produce greater definition between the two peaks in $\Delta E_2(x_{tip})$, allowing better resolution of the two peaks in $|\Psi_2(x)|^2$. This makes ultra-thin semiconductor nanowires a good system for wavefunction extraction, because the electrons are close to the surface.

The plots in Fig. 3 show that a longer quantum dot improves the ability of the tip to image spatial features in the wavefunction $\Psi(x)$. Increasing the dot length from L_{dot} = 300 nm in Figs. 3(a) to 3(c), to L_{dot} = 500 nm in Figs. 3(d) to 3(f) provides better resolution of the two peaks in $\Delta E_2(x_{tip})$ and the density profile $|\Psi_2(x)|^2$ of the dot. For example, visualization of the splitting between peaks in $\Delta E_2(x_{tip})$ is improved in Fig. 3(d) where L_{dot} = 500 nm compared with Fig. 3(a) where L_{dot} = 300 nm.

D. Measurement technique

The energy change $\Delta E(x_{tip})$ caused by denting the electronic wavefunction with the SPM tip as it is moved along the nanowire dot can be measured using Coulomb blockade spectroscopy. This energy change $\Delta E(x_{tip})$ shifts the position in backgate voltage V_{bg} at which a Coulomb blockade conductance peak occurs. By shifting V_{bg} in order to remain at the same point on a Coulomb blockade peak as the tip is scanned above the quantum dot, we can map $\Delta E(x_{tip})$ *vs*. tip position x_{tip} as described below.

Figure 4(a) is a graphical representation of the effect that the tip location has on the charge stability diagram of the quantum dot in the Coulomb blockade regime. The dotted parabolas in Fig. 4(a) show the electrostatic charging energy of the quantum dot $U_N = \left(C_{bg}V_{bg} - Ne\right)^2 \Big/ 2C_\Sigma$ when energy level spacing is small and no tip is present; here N is the number of electrons on the dot, C_{bg} is the capacitance between the backgate and the dot, and C_Σ is the total dot capacitance to ground. [34] Coulomb blockade conductance peaks, shown in Fig. 4(b) as the red (lighter) trace with no tip present, occur when the parabolas for N and $N + 1$ electrons intersect, because the energy of having N or $N + 1$ electrons on the dot is the same. As shown by the solid parabolas in Fig. 4(a), when the SPM tip is scanning a dot, the change in energy shifts each parabola upward by an amount $\Delta E_N(x_{tip})$, which is determined by the density profile $|\Psi(x)|^2$ as described above. The energy difference $\Delta E_{SN}(x_{tip})$ between two adjacent parabolas is given by:

$$\Delta E_{SN}(x_{tip}) = \Delta E_N(x_{tip}) - \Delta E_{N-1}(x_{tip}). \tag{8}$$

As shown in Fig. 4, the energy difference $\Delta E_{SN}(x_{tip})$ shifts the backgate voltage V_{bg} at which the two parabolas intersect and moves the corresponding Coulomb blockade peaks by an amount ΔV_{SN}, shown by the blue (darker) trace in Fig. 4(b): [35]

$$\Delta V_{SN}(x_{tip}) = \frac{C_{\Sigma}}{eC_{bg}}(\Delta E_N(x_{tip}) - \Delta E_{N-1}(x_{tip})). \quad (9)$$

The shift $\Delta V_{SN}(x_{tip})$ can be determined by Coulomb blockade measurements as described below.

Figure 5 illustrates the measurement technique. At the left is a schematic diagram showing the SPM tip scanned a distance H_{tip} above a nanowire quantum dot defined by two barriers. On the right is a series of Coulomb blockade conductance traces recorded at different locations x_{tip} along the dot. To the left of the Coulomb blockade peak, N = 0 and the dot is empty of electrons. To the right of the peak, an electron is added to the quantum dot. The position of each conductance peak is shifted by the difference $\Delta V_{SN}(x_{tip})$ between the energy states from denting the wavefunction. This shift can be recorded in the following way. The tip voltage is adjusted so that the conductance G_{sd} through the dot is halfway up a Coulomb blockade peak, shown by the red circle. As the tip is moved along the dot, the backgate voltage V_{bg} is adjusted by a feedback loop to keep G_{sd} halfway up the peak, as shown by the purple (dark) line $\Delta V_{SN}(x_{tip})$ in Fig. 5. By measuring the output $\Delta V_{SN}(x_{tip})$, we can find the difference in $\Delta E_N(x_{tip})$ from Eq. 9.

Figure 6 shows how the change in energy $\Delta E_N(x_{tip})$ of a single state can be found from the measured Coulomb blockade conductance peak shift $\Delta V_{SN}(x_{tip})$. From $\Delta E_N(x_{tip})$ we can extract the density profile of the wavefunction for that state $|\Psi_N(x)|^2$ using Eq. 7. The peak shift $\Delta V_{SN}(x_{tip})$ is proportional to the energy difference $\Delta E_N(x_{tip}) - \Delta E_{N-1}(x_{tip})$ between the N and $N+1$ peaks, as shown in Eq. 9. Figures 6(a) to 6(c) plot $\Delta E_N(x_{tip}) - \Delta E_{N-1}(x_{tip})$ for the first three Coulomb blockade peaks, going from $N = 0$ to $N = 3$. By assuming that $\Delta E_0(x_{tip}) = 0$ and

performing simple addition, the individual changes in energy $\Delta E_N(x_{tip})$, for the first three states of the dot, going from $N = 1$ to $N = 3$ are found, as shown in Figs. 6(d) to 6(f).

The final step needed to extract the density profile $|\Psi_N(x)|_{ext}^2$ of a wavefunction from the measured energy change is to use Eq. 7 to deconvolve $\Delta E_N(x_{tip})$ and the known tip potential $\Phi_{tip}(x - x_{tip})$. The extracted density profiles $|\Psi_N(x)|_{ext}^2$ obtained for $N = 1$ to $N = 3$, shown in Figs. 2(j) to 2(l) above, are in close agreement with the original density profiles $|\Psi_N(x)|^2$, shown in Figs. 2(a) to 2(c), that were entered into the analysis. Using this technique a cooled SPM can measure the energy E_N of an individual electron state and image the density profile $|\Psi_N(x)|^2$ of its wavefunction. Knowledge of the energy and wavefunctions of electron states buried inside a nanostructure promises to be extremely beneficial for the design of quantum devices for nanoelectronics or quantum information processing.

III. SUMMARY

We propose a novel SPM imaging technique that can extract the density profile of the wavefunction of an electron state in a quantum dot using a capacitive probe. A weakly charged SPM tip creates a small indentation in the wavefunction. By measuring the shift in Coulomb blockade peak position, as the SPM tip is moved along the quantum dot's length, the change in energy of the quantum state caused by the tip can be recorded. Using first-order perturbation theory, the density profile of the electronic wavefunction can be extracted from the SPM tip potential $\Phi_{tip}(x - x_{tip})$ and the measured change in energy $\Delta E_N(x_{tip})$ of the electron state. This technique compliments earlier methods to image the electron probability density in quantum

rings.[10-13] Access to this fundamental information about the electron system will advance designs and applications of quantum devices.

ACKNOWLEDGMENTS

We thank L. Samuelson, K. Storm, J. Berezovsky, H. Trodahl, and M. Stopa for helpful discussions. This research was supported at Harvard University by the NSF funded Nanoscale Science and Engineering Center (NSEC) under grant NSF/PHY06-46094.

REFERENCES

[1] E. J. Heller, M. F. Crommie, C. P. Lutz, and D. M. Eigler, Nature **369**, 464 (1994).

[2] H. C. Manoharan, C. P. Lutz, and D. M. Eigler, Nature **403**, 512 (2000).

[3] S. G. Lemay, J. W. Janssen, M. van den Hout, M. Mooij, M. J. Bronikowski, P. A. Willis, R. E. Smalley, L. P. Kouwenhoven, and C. Dekker, Nature **412**, 617 (2001).

[4] C. R. Moon, L. S. Mattos, B. K. Foster, G. Zeltzer, W. Ko, and H. C. Manoharan, Science **319**, 782 (2008).

[5] M. A. Topinka, R. M. Westervelt, and E. J. Heller, Phys. Today **56**, 47 (2003).

[6] A. E. Gildemeister, T. Ihn, R. Schleser, K. Ensslin, D. C. Driscoll, and A. C. Gossard, J. Appl. Phys. **102**, 083703 (2007).

[7] M. P. Jura, M. A. Topinka, L. Urban, A. Yazdani, H. Shtrikman, L. N. Pfieffer, K. W. West, and D. Goldhaber-Gordon, Nature Phys. **3**, 841 (2007).

[8] J. Berezovsky, M. F. Borunda, E. J. Heller, and R. M. Westervelt, Nanotechnology **21**, 274013 (2010).

[9] J. Berezovsky and R. M. Westervelt, Nanotechnology **21**, 274014 (2010).

[10] F. Martins, B. Hackens, M. G. Pala, T. Ouisse, H. Sellier, X. Wallart, S. Bollaert, A. Cappy, J. Chevrier, V. Bayot, and S. Huant, Phys. Rev. Lett. **99**, 136807 (2007).

[11] M. G. Pala, B. Hackens, F. Martins, H. Sellier, V. Bayot, S. Huant, and T. Ouisse, Phys. Rev. B **77**, 125310 (2008).

[12] B. Szafran, Phys. Rev B **84**, 075336 (2011).

[13] M. T. Woodside and P. L. McEuen, Science **296**, 1098 (2002).

[14] P. Fallahi, A. C. Bleszynski, R. M. Westervelt, J. Huang, J. D. Walls, E. J. Heller, M. Hanson, and A. C. Gossard, Nano Lett. **5**, 223 (2005).

[15] A. C. Bleszynski, F. A. Zwanenburg, R. M. Westervelt, A. L. Roest, E. P. A. M. Bakkers, and L. P. Kouwenhoven, Nano Lett. **7**, 2559 (2007).

[16] A. C. Bleszynski-Jayich, L. E. Fröberg, M. T. Björk, H. J. Trodahl, L. Samuelson, and R. M. Westervelt, Phys. Rev. B **77**, 245327 (2008).

[17] S. Schnez, J. Güttinger, M. Huefner, C. Stampfer, K. Ensslin, and T. Ihn, Phys. Rev. B **82**, 165445 (2010).

[18] E. E. Boyd, K. Storm, L. Samuelson, and R. M. Westervelt, Nanotechnology **22**, 185201 (2011).

[19] R. C. Ashoori, H. L. Stormer, J. S. Weiner, L. N. Pfeiffer, K. W. Baldwin, and K. W. West, Phys. Rev. Lett. **71**, 613 (1993).

[20] S. Tarucha, D. G. Austing, T. Honda, R. J. van der Hage, and L. P. Kouwenhoven, Phys. Rev. Lett. **77**, 3613 (1996).

[21] W. G. van der Wiel, S. De Franceschi, J. M. Elzerman, T. Fujisawa, S. Tarucha, and L. P. Kouwenhoven, Rev. Mod. Phys. **75**, 1 (2003).

[22] C. M. Lieber, MRS Bull. **28**, 486 (2003).

[23] B. J. Ohlsson, M. T. Björk, H. Magnusson, K. Deppert, L. Samuelson, and L. R. Wallenberg, Appl. Phys. Lett. **79**, 3335 (2001).

[24] M. T. Björk, B. J. Ohlsson, T. Sass, A. I. Persson, C. Thelander, M. H. Magnusson, K. Deppert, L. R. Wallenberg, and L. Samuelson, Appl. Phys. Lett. **80**, 1058 (2002).

[25] M. T. Björk, B. J. Ohlsson, T. Sass, A. I. Persson, C. Thelander, M. H. Magnusson, K. Deppert, L. R. Wallenberg, and L. Samuelson, Nano Lett. **2**, 87 (2002).

[26] A. Fuhrer, L. E. Fröberg, J. N. Pedersen, M. W. Larsson, A. Wacker, M. Pistol, and L. Samuelson, Nano Lett. **7**, 243 (2007).

[27] K. Ensslin, H. Baum, P. F. Hopkins, and A. C. Gossard, Surface Science **205**, 317 (1994).

[28] E. E. Vdovin, A. Levin, A. Patane, L. Eaves, P. C. Main, Y. N. Khanin, Y. V. Dubrovski, M. Henini, and G. Hill, Science **290**, 122 (2000).

[29] P. Fallahi, Ph.D. thesis, Harvard University, 2006.

[30] J. Qian, B. I. Halperin, and E. J. Heller, Phys. Rev. B **81**, 125323 (2010).

[31] M. A. Topinka, Ph.D. thesis, Harvard University, 2002.

[32] A. V. Oppenheim and A. S. Willsky, *Signals & Systems Second Edition* (Prentice Hall, Upper Saddle River, New Jersey, 1997).

[33] C. W. J. Beenakker, Phys. Rev. B **44**, 1646 (1991).

[34] M. Tinkham, *Introduction to Superconductivity* (McGraw-Hill, New York, 1996).

[35] C. W. J. Beenakker and H. van Houten, Solid State Physics **44**, 1 (1991).

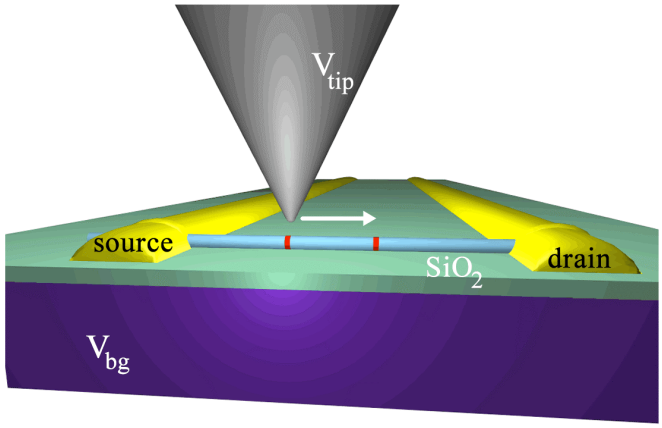

FIG. 1: Proposed experimental setup for extracting the electron's wavefunction. The charged SPM tip is scanned with a constant voltage V_{tip} with respect to the nanowire at a constant height H_{tip} in a straight line above the nanowire. The nanowire is deposited on a degenerately doped Si substrate that is topped with a SiO_2 thermal oxide. A backgate voltage V_{bg} is applied to the underside of the Si substrate to manipulate the charge state of the dot. The red (darker) segments of the nanowire represent tunnel barriers in an otherwise uniform nanowire. In this paper, to demonstrate the extraction technique, the quantum dot is approximated as a 1D quantum well with infinite sidewall potentials.

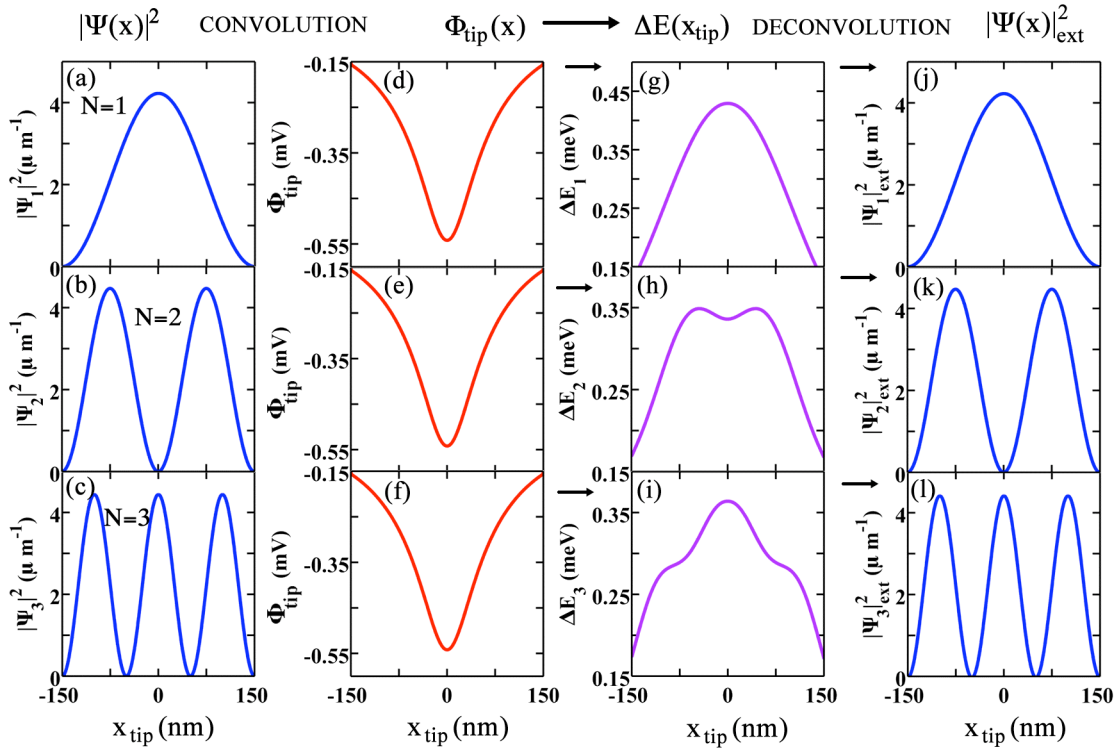

FIG. 2: Demonstration of extracting the amplitude of the wavefunction $|\Psi_{ext}(x)|^2$ for a nanowire with L_{dot} = 300 nm, d_{dot} = 30 nm, V_{tip} = -10 mV, l_{ox} = 10 nm, H_{tip} = 10 nm, and R_{tip} = 20 nm. (a)-(c) The normalized single particle wavefunction $|\Psi_N|^2$ for the first three states of an electron in a quantum well. (d)-(f) The tip potential Φ_{tip} modeled as a conducting sphere (Eq. 3, c = 0.64). (g)-(i) Convolving $|\Psi_N|^2$ with Φ_{tip} gives the change in energy of the dot ΔE_N as a function of tip position x_{tip}. (j)-(l) If $\Delta E_N(x_{tip})$ is measured from experiment and the shape of Φ_{tip} is well-known, ΔE can be deconvolved with Φ_{tip} to extract the amplitude of the wavefunction $|\Psi_{ext}|^2$.

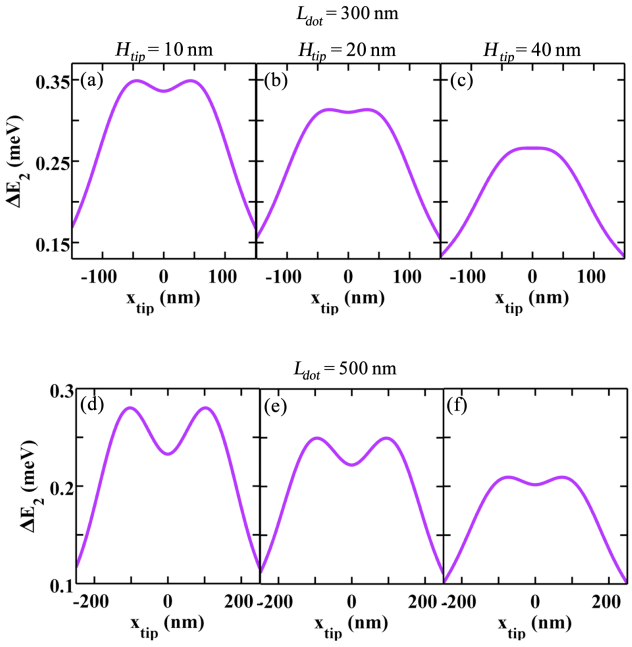

FIG. 3: The change in $\Delta E_2(x_{tip})$ for a variety of values of H_{tip} and L_{dot} (d_{dot} = 30 nm). (a)-(c) & (d)-(f) Decreasing the separation H_{tip} between the nanowire and the tip (R_{tip} = 20 nm) for a given L_{dot} gives a sharper tip potential, which increases the similarity of $\Delta E_2(x_{tip})$ to $|\Psi_2|^2$. Likewise, increasing the dot length L_{dot} also improves the clarity of the features of $|\Psi_2|^2$.

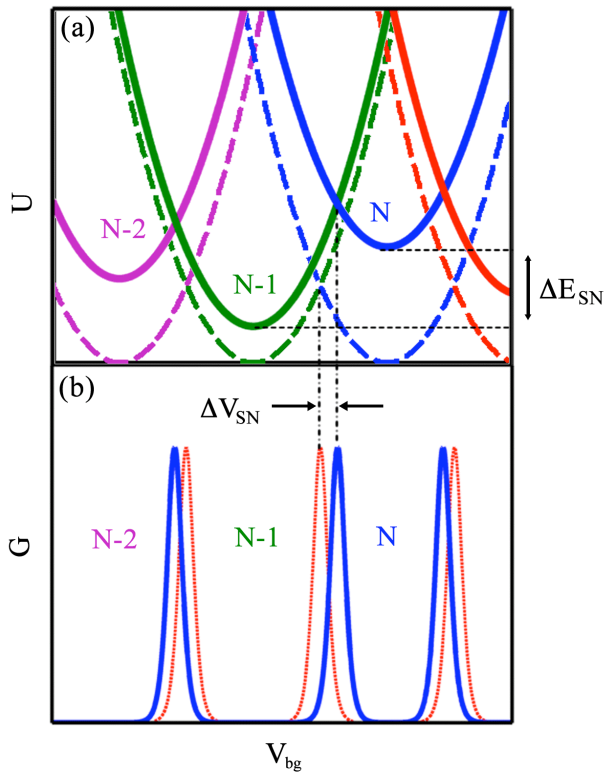

FIG. 4: (a) Free energy *U vs*. backgate voltage V_{bg}. The dashed parabolas are the electrostatic energy when the single particle energy levels can be neglected and no tip is present. The number of electrons on the dot changes by one when the dashed parabolas intersect. N, N - 1, N - 2 represent the number of electrons on the dot. The solid parabolas are the free energy of the dot, when the tip changes the energy of the dot by $\Delta E_N(x_{tip})$. This interaction shifts the parabolas up in U by $\Delta E_N(x_{tip})$ and shifts the intersection of the parabolas along the V_{bg} axis. (b) The shift changes the location of the Coulomb blockade conductance peaks as shown in Eq. 9. The red (lighter color) dotted Coulomb blockade peaks correspond to the intersections of the dashed energy parabolas when no tip is present. The blue (darker color) solid Coulomb blockade peaks show the shift in V_{bg} of the Coulomb blockade peaks with the tip present. The change in Coulomb blockade peak spacing $\Delta V_{SN}(x_{tip})$ due to the tip is proportional to the difference in the change in energy of two states due to the tip position: $\Delta V_{SN}(x_{tip}) \propto \Delta E_N(x_{tip}) - \Delta E_{N-1}(x_{tip})$.

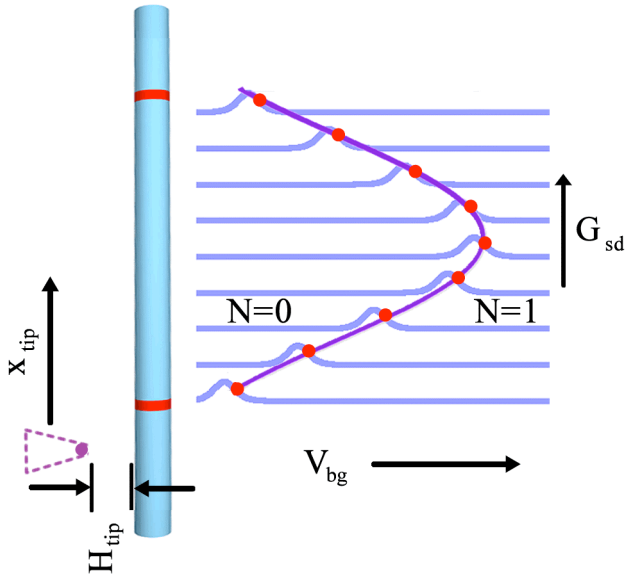

FIG. 5: Illustration of the transition between $N = 0$ and $N = 1$ on the quantum dot. The tip is scanned at height H_{tip} in a straight line along the length of the quantum dot x_{tip}. The blue (lighter) traces to the right show the Coulomb blockade conductance peak, where it is equally energetically favorable for the dot to hold either 0 or 1 electrons. As the tip changes its location x_{tip}, the backgate voltage V_{bg} the peak occurs at shifts. The red dots mark the same value of conductance for each tip position x_{tip}. The purple (darker) line traces how V_{bg} must vary in order to keep the conductance G_{sd} of the nanowire constant. The change in backgate voltage $\Delta V_{SN}(x_{tip})$, purple (darker) line, is proportional to $\Delta E_3(x_{tip}) - \Delta E_2(x_{tip})$.

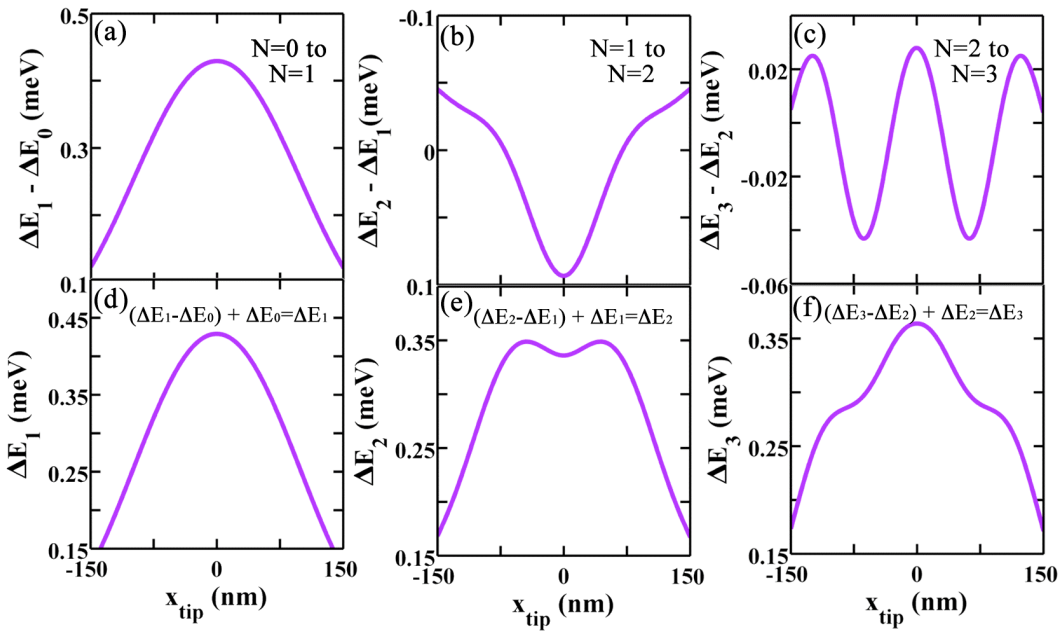

FIG. 6: (a)-(c) Shows the difference in the change of energy $\Delta E_N(x_{tip}) - \Delta E_{N-1}(x_{tip})$ of quantum states of a dot for N = 1 to 3, which is proportional to change in backgate voltage V_{bg} needed to keep the conductance G_{sd} through the nanowire constant. This model has a nanowire and a tip with L_{dot} = 300 nm, d_{dot} = 30 nm, V_{tip} = -10 mV, H_{tip} = 10 nm, and R_{tip} = 20 nm. (d)-(f) Assuming that $\Delta E_0(x_{tip}) = 0$, gives $\Delta E_1(x_{tip}) - \Delta E_0(x_{tip}) = \Delta E_1(x_{tip})$ as seen in (d). Likewise, using simple addition $\Delta E_2(x_{tip})$ and $\Delta E_3(x_{tip})$ are also found in (e) and (f) $[(\Delta E_2(x_{tip}) - \Delta E_1(x_{tip})) + \Delta E_1(x_{tip}) = \Delta E_2(x_{tip})$ $(\Delta E_3(x_{tip}) - \Delta E_2(x_{tip})) + \Delta E_2(x_{tip}) = \Delta E_3(x_{tip})]$. The $\Delta E_N(x_{tip})$ in (d)-(f) can be deconvolved with $\Phi_{tip}(x-x_{tip})$ to extract the amplitude of the wavefunction $|\Psi_{ext}|^2$ as shown in Fig. 2.